HN$_2$(^{2}A′) Electronic Manifold. I. A Global ab Initio Study of First Two States†

Vinícius C. Mota and António J.C. Varandas*

Departamento de Química, Universidade de Coimbra, 3004-535 Coimbra, Portugal

Received: January 12, 2007

A detailed ab initio multireference configuration interaction calculation with a standard aug-cc-pVTZ basis set is reported for the 1^{2}A′ and 2^{2}A′ states of the title system. The aim is to establish the dissociation scheme of all channels, while revealing the 2^{2}A′/3^{2}A′ seam of conical intersections consistent with the crossings in the diatomic fragments. An ab initio mapping of linear NNH and T-shaped and linear NHN loci of conical intersections is also reported, jointly with a discussion of the topological features associated to a newly reported 2^{2}A′/3^{2}A′ crossing seam.

1. Introduction

Since Miler and co-workers[1] postulated that HN$_2$ + OH might be an important product of the reaction

$$NH_2 + NO \rightarrow \text{products} \qquad (1)$$

which is a primary step on the thermal De−NO$_x$ processes, a large effort has been made toward the direct observation of HN$_2$. Theoretically, such an effort has assumed mostly the form of electronic structure calculations and dynamics to determine a reliable lifetime of the HN$_2$ intermediate complex.

In 1989, Walch et al.[2] reported the first multireference contracted configuration interaction calculations including single and double electron excitations using a complete-active-space wave function (CASSCF/CCI) as reference and an atomic natural orbital (ANO) basis set. Such a study provided an improved global description of the relevant potential energy surfaces (PESs) over earlier single-reference calculations by Curtiss et al.[3] From the calculated minimum energy path, they have estimated[2] the lifetime of HN$_2$ to lie between 10^{-11} s and 10^{-9} s. After some basis set improvement, Walch[4] has reported a grid of 250 points and a global seminumerical PES[5] for the title system. A lifetime of 3×10^{-9} s was then obtained for the HN$_2$ intermediate from dynamics calculations on such a PES, thus revealing good accord with the earlier estimate by the same group. By extrapolating to the one-electron infinite basis set limit, Walch and Partridge[6] have subsequently reported a small raising of 0.1 kcal mol^{-1} in the dissociation barrier height. They have obtained for this barrier a value of 11.3 kcal mol^{-1}, which led them to restate confidence on the earlier reported lifetime.[5] Furthermore, by employing high-level coupled-cluster singles and doubles theory as well as the perturbative triples correction in CCSD(T) calculations with a standard[7] augmented correlation consistent basis set of Dunning's[7,8] aug-cc-pVQZ type (heretofore denoted by AVQZ) basis set, Gu et al.[9] reported values of 10.7 and 3.8 kcal mol^{-1} for the barrier height to dissociation and exothermicity, respectively, suggesting that the lifetime of the HN$_2$ complex could be even smaller. Motivated by this result, Poveda and Varandas[10] have reported a global PES based on a grid of 900 MRCI/AVQZ energies which have been scaled

using the double many-body expansion scaled external correlation[11] (DMBE-SEC) method. From their work,[10] a dissociation barrier height of 10.6 kcal mol^{-1} has been predicted, thus supporting an even shorter lifetime for the HN$_2$ complex, as indeed confirmed by subsequent dynamics calculations.[12,13]

In addition to the ground-state studies reported in the previous paragraph, there have been investigations on the excited-states of the title system.[14−18] Selgren et al.[15] employed a neutralization−reionization process over HN$_2^+$ ion beams that could detect the HN$_2$ radical if its lifetime were larger than a threshold of 5×10^{-7} s. Having failed in their experimental attempt to observe this radical, they supported the available[3] theoretical predictions of HN$_2$ lifetimes 2−4 orders of magnitude smaller than the above threshold value. However, their measurements of the kinetic energy released from HN$_2^+$ + K fragmentation raised the possibility of detection of such a species through radiation from its excited states. On the basis of calculations of electronic transitions by Vasudevan et al.[14] and some local single-reference Moller−Plesset perturbation theory (MP4) calculations for the ^{2}A′ and ^{2}A″ states with a 6-311G** basis set and diffuse functions, Selgren et al.[15] have then suggested that the 3s-Rydberg states might be near resonant with the HN$_2^+$ + K states, thus pointing that "transitions from an upper $n = 3$ Rydberg level to the lower ^{2}A′ and ^{2}A″(Π) levels might constitute the first spectroscopic observation of the radical". Inspired by such a possibility, Walch[16] has performed CASSCF/CCI calculations, employing diffuse functions in the basis sets for the linear components of both the ^{2}A′ and ^{2}A″ states, including 2^{2}A′ and an optimized $n = 3$ Rydberg states. These more accurate calculations have shown[16] that the Rydberg states were in fact out of the range for resonance with HN$_2^+$ + K by more than 1 eV, although excited vibrational states supported by 2^{2}A′ not only were lying in a favorable range of energies but might present favorable Franck−Condon factors with lower vibrational levels of ^{2}A″.

Besides suggesting that further investigations on both the ground and excited states of the title system are welcome, especially for the excited state, the previous paragraphs reveal that a global description of the manifold of coupled electronic states is unavailable thus far. Encouraged by the accuracy achieved for the PES of ground-state HN$_2$ through the DMBE-SEC[11] method, we report in the present work an ab initio study of the first two coupled states of A′ symmetry over the full

---

dimensional space of HN_2. While this provides raw data for modeling a double-sheeted PES for the title radical using DMBE[19] theory, we focus here on the dissociative behavior of the excited states (section 3) and the involved conical intersections (section 4).

2. Ab Initio Calculations.

All ab initio calculations have been carried out at the MRCI[20] level using the full-valence CAS[21] wave function (FVCAS) as reference. Because of the existence of conical intersections between the excited states, we have carried out state-averaged FVCAS calculations including more than two states. This warranted both convergence to the correct states and a smooth behavior of the PESs in the neighborhood of geometries where the $2^2A'$ state becomes degenerate with the next state of the same symmetry. At some regions, dense-grid calculations have also been performed to elucidate the shape of the electronic manifold, a crucial step for the subsequent DMBE[19] modeling. Such requirements led us to reduce as much as possible the computational cost by limiting the one-electron basis set size. A convenient choice has been the AVTZ basis set, with all correlated calculations being carried out with the MOLPRO[22] package. To compensate for deficiencies due to incompleteness of the one-electron basis set and truncation of the CI expansion, such energies will be corrected prior to the modeling procedure by using the DMBE-scaled external-correlation (DMBE-SEC[11]) method.

Despite focusing in specific regions of configuration space, mostly to determine crossing seams and establish dissociative patterns, the results described in the present work involve nearly 3000 geometries that allow a full mapping of the first two electronic states. The covered regions are defined by $0.0 \leq r_{N_2}/a_0 \leq 4.4$, $0.0 \leq R_{H-N_2}/a_0 \leq 10.0$, and $0 \leq \gamma/deg \leq 90$ for $H-N_2$ interactions and $0.0 \leq r_{NH}/a_0 \leq 3.3$, $1.0 \leq R_{N-NH}/a_0 \leq 6.0$, and $0 \leq \gamma/deg \leq 180$ for $N-NH$ interactions; r, R, and γ are the corresponding atom−diatom Jacobi coordinates. All calculated energies will be referred to the full atomization energy of the ground electronic state.

3. Dissociation Scheme

The analysis of the dissociation pattern for the $^2A'$ states of HN_2 is a crucial step toward the modeling of a global PES via many-body expansion[19,23−25] techniques, which has been done thus far only for the ground electronic state:[5,10]

$$HN_2(1^2A') \rightarrow \begin{cases} N_2(^1\Sigma_g^+) + H(^2S) \\ NH(^3\Sigma^-) + N(^4S), \end{cases} \quad (2)$$
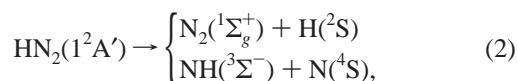
where both channels lead to the products $2N(^4S) + H(^2S)$. For the first excited-state of $^2A'$ symmetry, a complete dissociation scheme such as in eq 2 has not yet been established, with calculations for the $H-N_2$ channel being, to our knowledge, the only ones available in the literature.[14,16,18]

Walch[16] has reported calculations for the $1^2A'$, $2^2A'$, and $^2A''$ PESs at regions of configuration space in the neighborhood of the linear $^2\Sigma$ /$^2\Pi$ ($1^2A'/2^2A'$ in C_s symmetry) conical intersection. In his work, the r_{NN} and θ_{HNN} coordinates have been fixed at $2.1a_0$ and $180°$, respectively, with energy profiles being generated for $2.0 \leq r_{NH}/a_0 \leq 5.0$. Over this region, the $^2\Sigma$ and $^2\Pi$ states are identified as the linear components of both $1^2A'$, $2^2A'$, and $^2A''$ states, although the lack of calculations for larger r_{NH} values prevents any conclusive results about the dissociation products. Based on symmetry arguments, Walch has established $N_2(^1\Sigma_g^+) + H(^2S)$ to be the dissociation products of the $^2\Sigma$

state, and $N_2(^3\Pi_g) + H(^2S)$ of the $^2\Pi$ state. In turn, Vasudevan et al.[14] have shown that dissociation of the $^2\Sigma$ state is the same as for $1^2A'$, but no calculations have been reported thus far to relate the dissociations of the $^2\Pi$, $2^2A'$, and $^2A''$ states.

Following an experimental study of the reaction $N_2(^3\Sigma_u^+) + H(^2S)$,[17] Sperlein and Golde[18] have carried out an ab initio study of HN_2 in the neighborhood of T-shaped configurations aiming at clarifying the insertion mechanism of $H(^2S)$ into N_2. For T-shaped configurations, the r_{NN} coordinate of the triatomic assumed values close to the experimental equilibrium geometry of the N_2 fragment while, for configurations of both ground and excited electronic states of HN_2 with C_s symmetry, it was set equal to the equilibrium $N_2(^1\Sigma_g^+)$ geometry. More precisely, for the T-shaped $^2B_2$ state, which correlates with $N_2(^3\Sigma_u^+)$ at its equilibrium geometry[26] ($r_{NN} = 2.432a_0$), values ranging from $2.148a_0$ to $2.432a_0$ have been considered, while for the T-shaped $^2A_1$ state, which correlates with $N_2(^1\Sigma_g^+)$ at its equilibrium geometry ($r_{NN} = 2.074a_0$), such separations range from $1.980a_0$ to $2.074a_0$. For all such geometries, the calculations demonstrate that both the $^2B_2$ and $2^2A'$ states correlate via the same dissociation channel: $N_2(^3\Sigma_u^+) + H(^2S)$.

From the above, it is clear that results have been reported only for $2.074 \leq r_{NN}/a_0 \leq 2.432$, thus highlighting the need for further calculations, in particular for linear arrangements of the triatomic system close to dissociation. This can be seen from our calculations, which are depicted in Figure 1 (top row) for linear ($\theta_{HNN} = 180°$) geometries at three r_{NN} distances and a wide range of R_{H-NN} values. Some ab initio points for fixed r_{NN} values at $\theta_{HNN} = 165°$ are also included. As seen, our results indicate the existence of a seam of conical intersection between the $2^2A'$ and $3^2A'$ states which, to our knowledge, had not been identified before. As it will be shown, this corresponds at linear geometries to the crossing of the $^2\Pi$ and $2^2\Sigma$ states.

The possibility of such a crossing requires a higher level of detail for understanding the corresponding dissociation channels. Panel a of Figure 2 shows three sets of calculations for the $H-N_2$ dissociation as a function of r_{NN}. Two such sets correspond to linear and T-shaped arrangements, with the H atom fixed at a distance of $10a_0$ from the geometric center of the diatomic. The third set refers to arrangements with C_s symmetry, with the H atom fixed at a distance of $15a_0$ from the geometric center of N_2, and the atom−diatom vector forming with the diatomic axis an angle of $15°$. These fixed R_{H-N_2} distances were chosen to be sufficiently large to minimize the $H-N_2$ interaction but small enough to ensure proper convergence of the many-state ab initio calculations. The following discussion focuses on the qualitative trends of such "diatomic-like" potentials, thus ignoring for this matter the influence of the $H-N_2$ interaction. We emphasize the existence of conical intersections between the first and second excited states, which produces strong couplings and hence imposes consideration of the second and higher excited states to correctly identify the first excited one. In fact, a six-state FVCAS calculation has been found necessary near such crossings before the two-state MRCI curves could reliably describe the involved PESs.

From the potential curves for the low-lying bound states of N_2 (ref 27 and references therein), our calculations show that the $2^2\Sigma$ (linear), $^2B_2$ (T-shaped), and $2^2A'$ (C_s) states share the same dissociation products, $N_2(^3\Sigma_u^+) + H(^2S)$, from a value of $r_{NN} = 2.074a_0$ up to full atomization. However, for r_{NN} distances smaller than $2.074a_0$, the situation requires more attention. As panel a of Figure 1 shows, for $r_{NN} = 1.854a_0$, the $2^2\Sigma$ and $^2\Pi$ (linear) states do not intersect. In turn, the insert in panel a of Figure 2 shows that the linear triatomic states reproduce the
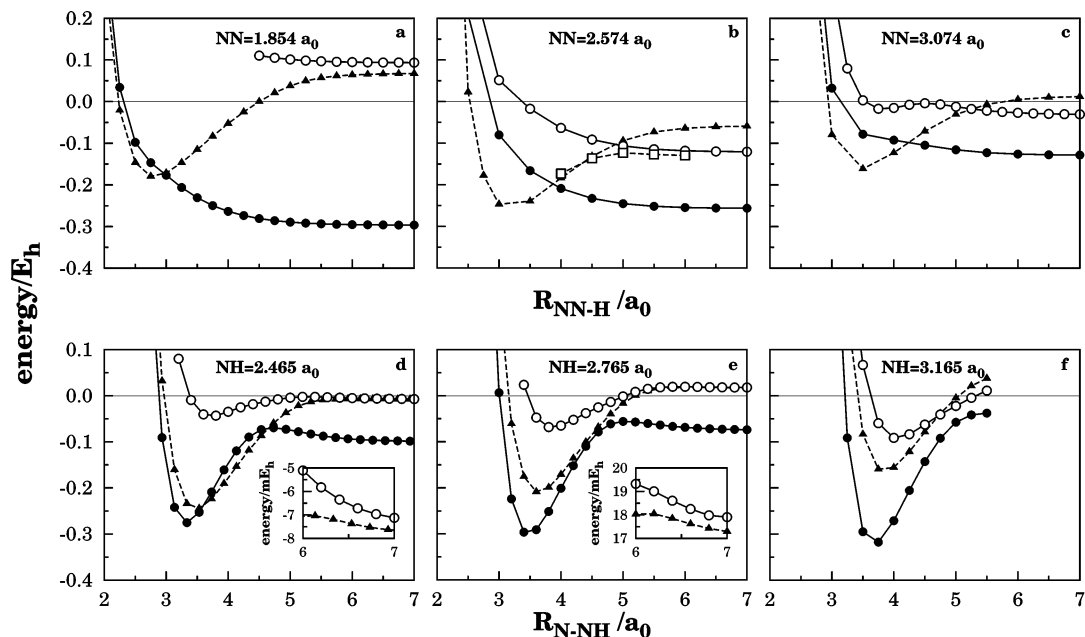
Figure 1. $1^2\Pi/2^2\Sigma$ crossing seam along selected linear geometries: (●) $1^2\Sigma$, (○) $2^2\Sigma$, (▲) $1^2\Pi$, (□) 2^2A′ with $\theta_{\text{HNN}} = 165°$. For the H + N$_2$ channel, the $2^2\Sigma$ and $^2\Pi$ states dissociate to N$_2$($^3\Sigma_u^+$) + H(^{2}S) and N$_2$($^3\Pi_g$) + H(^{2}S), respectively, while for the channel N + NH the corresponding dissociation limits are NH($^5\Sigma$) + N(^{4}S) and NH($^3\Sigma^-$) + N(^{2}D). The lines between the points were drawn to guide the eye.
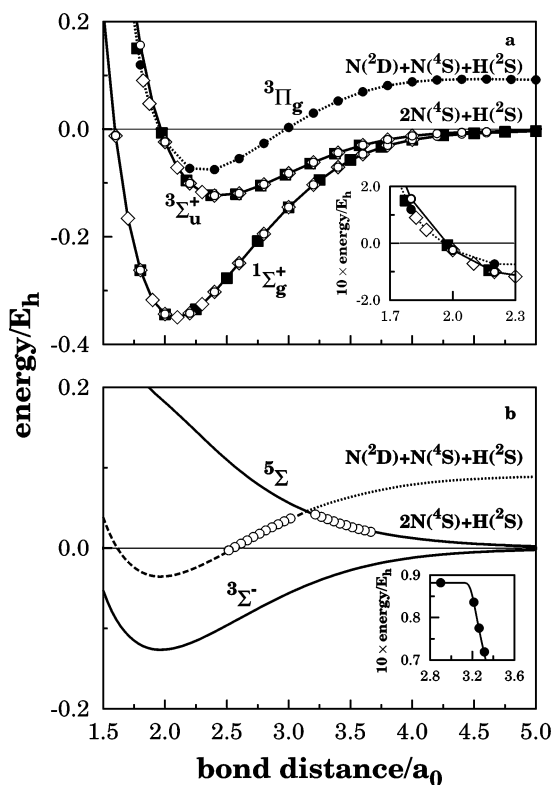
Figure 2. Asymptotic behavior in HN$_2$ at atom−diatom dissociations. In all panels, the symbols indicate the calculated triatomic energies. Key for $^3\Pi_g$ in panel a: (●) $^2\Pi$, (■) ^{2}B$_2$, (◇) 2^2A′. Key for $^3\Sigma_u^+$: (■) ^{2}B$_2$, (○) $2^2\Sigma$, (◇) 2^2A′. Key for $^1\Sigma_g^+$: (■) ^{2}A$_1$, (○) $1^2\Sigma$, (◇) 1^2A′. Solid and dashed lines connect the calculated points. Panel b shows the N−NH channel as a function of r_{NH}, with the solid lines indicating splines for NH($^3\Sigma^-$) and NH($^5\Sigma$) and the open circles (○) representing the energies for HN$_2$(^{2}A′). The dashed line indicates the calculations for the NH($^3\Sigma^-$) diatomic shifted by the [N(^{2}D) − N(^{4}S)] energy difference while the dotted one shows its analytic continuation (see the text).

crossing between the diatomic states N$_2$($^3\Sigma_u^+$) and N$_2$($^3\Pi_g$) at x_c ≈ 1.95a_0 (this is confirmed by our own MRCI calculations on
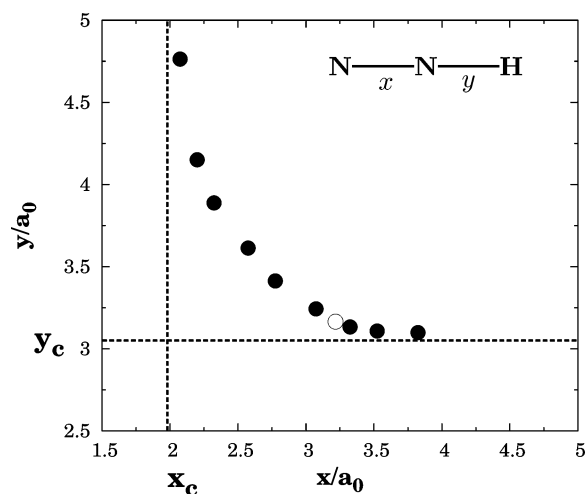
Figure 3. The $2^2\Sigma/^2\Pi$ linear conical intersection in HN$_2$. The solid dots denote calculations on the H−N$_2$ channel, while the open circles refer to N−NH. x_c and y_c indicate the coordinates of the crossing at the atom−diatom asymptotes.

such diatomic states and other available theoretical results[28]). We further observe from this panel that such a crossing at linear geometries becomes avoided at C_s and C_{2v} ones (cf. solid squares and diamonds in panel a of Figure 2).

The existence of the above 2^2A′/3^2A′ crossing is then consistent with crossings on the involved diatomic fragments at the H−N$_2$ channel. Further calculations have then been carried out to map this seam of linear 2^2A′/3^2A′ conical intersections at more compact linear geometries as exhibited in Figure 3. All major trends of such a crossing are depicted in this (x,y)-plot. For example, the 2^2A′/3^2A′ intersection shown in Figure 1 can be easily identified from the corresponding x and y cuts in Figure 3, as well as the configuration-space regions where they become avoided.

For the excited N−NH channel, we have not found any recent studies in the literature, although some preliminary calculations have shown a nontrivial behavior on dissociation. Panel b of Figure 2 illustrates the results of a detailed calculation for this

channel. In the plot, we have fixed $r_{NN} = 8.0a_0$, with the bond axis forming an angle of $\theta_{HNN} = 175°$ with H. To ensure convergence to the proper states, a dense grid of points has been constructed using six-state-averaged FVCAS calculations as also done in the H−N$_2$ case. Such a procedure was key in obtaining two-state properly converged results in the vicinity of the $2^2A'$/$3^2A'$ crossing seam. With a smaller number of states, the avoided crossing regions displayed irregularities and jumps between states.

Shown by the solid lines in panel b of Figure 2 are the $^3\Sigma^-$ (bound) and $^5\Sigma$ (unbound) states of NH. Also shown by the dashed line is the triatomic state predicted by energy-shifting the NH($^3\Sigma^-$) curve by $\delta_{NH} = N(^2D) - N(^4S)$, with the extrapolation up to dissociation being indicated by the dotted line. Clearly, up to the critical separation $y_c \approx 3.1a_0$ shown in Figure 3, the ab initio results indicate that the excited triatomic states dissociate to NH($^3\Sigma^-$) + N(^2D); for values in the vicinity of y_c, the points exhibit a crossing behavior, dropping from there onward into the NH($^5\Sigma$) + N(^4S) dissociation channel. Similar results can be found in the literature for other systems, for example, for C, N, and O inserting into H$_2$($^1\Sigma_g^+$).[29,30] Of course, an accurate description of such a behavior for the title system would imply consideration of the first three electronic states. In a simplifying attempt, Varandas and Poveda[31] have recently suggested a simple scheme to replace the crossing in the N−HH channel of NH$_2$ (where at $r_{HH} \approx 3.0a_0$ a change occurs from H$_2$($^1\Sigma_g^+$) + N(^2D) to H$_2$($^3\Sigma_u^+$) + N(^4S)) by a narrowly avoided one through the use of a switching function in the r_{HH} coordinate. Under the perspective of adopting a similar treatment for the HN−N channel, we show in the insert of panel b of Figure 2 a similar fit to the ab initio points that describes accurately the involved switching pattern. Details of this and other aspects of the modeling will be presented in a forthcoming publication, where a full three-dimensional two-sheeted DMBE potential energy surface will be reported.

4. Crossing Seams

A study of T-shaped and NNH linear conical intersections between the first two A′ states of HN$_2$ has been previously reported by Walch.[5,16] However, in his global PES such intersections have been replaced by narrowly avoided crossings.[5] Poveda and Varandas[10] followed a similar approach in modeling their own DMBE PES. Thus, no detailed topological features about the crossing seams can be extracted from previous work.[5,10,16] Sperlein and Golde[18] limited themselves to a local analysis of the avoided crossing behavior for T-shaped configurations and argue over its MO justification following the treatment employed by Vasudevan et al.[14] for the NNH linear crossing. However, these authors[14] have only considered r_{NN} separations close to equilibrium. Moreover, they have noted[14] the impossibility of using single-reference SCF calculations to describe the dissociation of excited states, which limited their capability to study the evolution of the NNH crossing seams. Also, and perhaps most important, they have not allowed for the possibility of a $2^2A'$/$3^2A'$ conical intersection, which would have introduced an unexpected pattern on dissociation. As for higher excited states, no previous detailed investigation of conical intersections has to our knowledge been reported, especially on their behavior toward dissociation.

Figure 4 shows the locus of conical intersections between the first two $^2A'$ states through (x,y) representations as well as the triatomic geometries assumed in each case. Panel a illustrates the T-shaped crossing seam. It starts at a linear NHN geometry with characteristic bond distance $x \approx 1.7a_0$ (marked in panel c
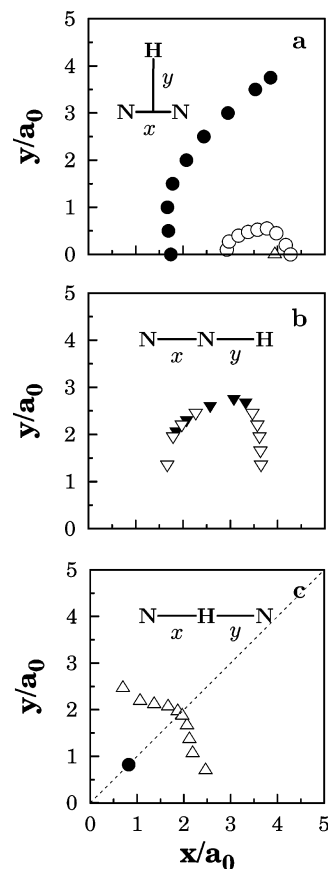
Figure 4. Panel a shows the calculated C_{2v} crossing points (●) for NN−H channel, with the small open circles indicating the T-shaped 2^2B_2/1^2A_1 conical intersection, and the open triangle the $D_{\infty h}$ crossing (see text). Panel b shows calculated linear NNH points: (▼) NN−H channel; (▽) HN−N channel. Panel c shows the calculated linear NHN points (△) with the $D_{\infty h}$ crossing being indicated by ●.

by a solid dot), and seems to continue up to the atomization asymptote of the $^2A'$ states. However, as the coordinates relax beyond 4 or 5a_0, the state-averaged calculations started to exhibit convergence problems, which prevented a study of the remaining locus. Panel a of Figure 2 reveals that the two $^2A'$ states become asymptotically degenerate, which suggests that the crossing seam in panel a of Figure 4 extends up to infinitely large C_{2v} structures, a situation often met in systems where the crossing is dictated by symmetry reasons.

Also seen in panel a of Figure 4 is an additional complication detected when modeling the first two $^2A'$ states of HN$_2$. It refers to a T-shaped seam of conical intersections between the $2^2A'$ and $3^2A'$ states for $R_{H−N_2}/a_0 < 0.6$ and $2.8 < r_{N_2}/a_0 < 4.4$, which have been confirmed via the Longuet−Higgins[32] topological theorem as first done in ref 33 for the LiNaK system. Such intersections appear far from any stationary point of the ground state, but its mapping has been key to identify the T-shaped triatomic states $^2B_2$ and $^2A_1$ as well as the linear triatomic states $^2\Sigma$ and $^2\Pi$ which should also be described when modeling globally the first two $^2A'$ states of the title system.
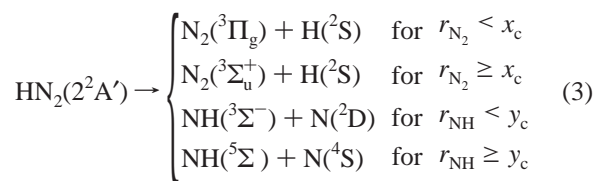
The linear crossings are shown in panels b and c of Figure 4. Only the ab initio points where convergence has been attained are indicated. For NNH linear configurations, the regions defined by $y \leq 1.0a_0$ or $x \leq 1.0a_0$ (where the potential becomes highly repulsive) could not be investigated at the ab initio level of theory employed in the present work. The same applies in panel c of Figure 4 for regions where $y \leq 0.5a_0$ or $x \leq 0.5a_0$. However, such regions are of minor practical interest as they sit on highly repulsive regions of the atom−diatom dissociation channels.

Also visible from panel b of Figure 4 are two distinct intersections along the HN$-$N channel. Such a result is also apparent from panel d of Figure 1 with $r_{NH} = 2.465a_0$. Panels e and f of Figure 1 also confirm the absence of any intersection for distances larger than about $r_{NH} = 2.75a_0$, as demonstrated by panel b of Figure 4. In fact, by looking at cuts for fixed x values, we observe the existence of at most a single crossing point, as confirmed by panels a, b, and c of Figure 1. On the basis of our converged calculations, it may be summarized that no more than two conical intersections occur along x for a fixed value of y, with only one intersection along y for a fixed x value.

The NHN seam of linear conical intersections is shown in panel c of Figure 4, where the diagonal ($D_{\infty h}$) line in dotted divides the regions related by permutation symmetry. For $y >$ 2.7a_0 and $x > 0.5a_0$, no crossings have been observed (this cannot be warranted for x values shorter than 0.5a_0 where the calculations could not be converged). The same applies by symmetry for regions defined by $x > 2.7a_0$ and $y > 0.5a_0$. Thus, the crossing seam appears to be delimited by $x,y < 2.7a_0$. Note that the dividing line in panel c contains crossings from two distinct seams. The seam shown by triangles refers to molecular arrangements with both $C_{\infty v}$ and $D_{\infty h}$ (only one point) symmetries. The crossing shown by the solid dot belongs to the C_{2v} seam in panel a for a zero atom$-$diatom separation ($y =$ 0). Similarly, the $C_{\infty v}$ seam maps its middle point with $D_{\infty h}$ symmetry onto the C_{2v} map of panel a as indicated by the open triangle. On the lack of a topological proof for linear geometries, such degeneracies have been confirmed up to $10^{-8}E_h$ in the state-averaged MCSCF calculations. Note that the common points to panels a and c indicate that two crossing seams are isolated (i.e., do not intersect each other); for papers referring to intersecting crossing seams, see refs 34 and 35.

5. Concluding Remarks

We have reported detailed ab initio calculations for the $1^2A'/2^2A'$ states of HN$_2$. They have shown a novel linear seam of conical intersections between the $2^2A'/3^2A'$ states which is related to crossings in the diatomic fragments. As a result, a global description of the $^2A'$ electronic manifold for the title system implies the following nontrivial dissociation scheme for the excited state:

$$HN_2(2^2A') \rightarrow \begin{cases} N_2(^3\Pi_g) + H(^2S) & \text{for } r_{N_2} < x_c \\ N_2(^3\Sigma_u^+) + H(^2S) & \text{for } r_{N_2} \geq x_c \\ NH(^3\Sigma^-) + N(^2D) & \text{for } r_{NH} < y_c \\ NH(^5\Sigma) + N(^4S) & \text{for } r_{NH} \geq y_c \end{cases} \quad (3)$$

where r_{N_2} is the Jacobi coordinate for the H$-$N$_2$ channel, r_{NH} is the corresponding coordinate for the N$-$NH channel, and (x_c,y_c) are the coordinates shown in Figure 3.

Sperlein and Golde[18] have reported difficulties in converging their two-state calculations, and considering the geometries they employed we can state that previous knowledge of the $2^2A'/3^2A'$ linear conical intersections might have helped to overcome the problem, mainly via addition of further $^2A'$ excited states on their CASSCF calculations. In fact, the first excited-state has shown a rather complicated topology, with at least a second crossing seam involving the third $^2A'$ excited-state at

T-shape configurations, as shown by the open circles in panel a of Figure 4.

In summary, we paved the way for the global modeling of the two first states of the $^2A'$ electronic manifold of HN$_2$ by computing over 6000 ab initio energies at the MRCI/AVTZ level, with emphasis on the involved crossing seams. The modeling is now complete and will hopefully be soon reported.

References and Notes

(1) Miller, J. A.; Branch, M. C.; Kee, R. J. *Combust. Flame* **1981**, *43*, 81.

(2) Walch, S. P.; Duchovic, R. J.; Rohlfing, C. M. *J. Chem. Phys.* **1989**, *90*, 3230.

(3) Curtiss, L. A.; Drapcho, D. L.; Pople, J. A. *Chem. Phys. Lett.* **1984**, *103*, 437.

(4) Walch, S. P. *J. Chem. Phys.* **1990**, *93*, 2384.

(5) Koizumi, H.; Schatz, G. C.; Walch, S. P. *J. Chem. Phys.* **1991**, *95*, 4130.

(6) Walch, S. P.; Partridge, H. *Chem. Phys. Lett.* **1995**, *233*, 331.

(7) Dunning, T. H., Jr. *J. Chem. Phys.* **1989**, *90*, 1007.

(8) Kendall, R. A.; Dunning, T. H., Jr.; Harrison, R. J. *J. Chem. Phys.* **1992**, *96*, 6796.

(9) Gu, J.; Xie, Y.; Schaefer, H. F., III. *J. Chem. Phys.* **1998**, *108*, 8029.

(10) Poveda, L. A.; Varandas, A. J. C. *J. Phys. Chem. A* **2003**, *107*, 7923.

(11) Varandas, A. J. C. *J. Chem. Phys.* **1989**, *90*, 4379.

(12) Caridade, P. J. S. B.; Rodrigues, S. P. J.; Sousa, F.; Varandas, A. J. C. *J. Phys. Chem. A* **2005**, *109*, 2356.

(13) Caridade, P. J. S. B.; Poveda, L. A.; Rodrigues, S. P. J.; Varandas, A. J. C. *J. Phys. Chem. A* **2007**, *111*, 1172.

(14) Vasudevan, K.; Peyerimhoff, S. D.; Buenker, R. J. *J. Mol. Struct.* **1975**, *29*, 285.

(15) Selgren, S. F.; McLoughlin, P. W.; Gellene, G. I. *J. Chem. Phys.* **1989**, *90*, 1624.

(16) Walch, S. P. *J. Chem. Phys.* **1991**, *95*, 4277.

(17) Ho, G. H.; Golde, M. F. *J. Chem. Phys.* **1991**, *95*, 8866.

(18) Sperlein, R. F.; Golde, M. F. *J. Chem. Phys.* **1991**, *95*, 8871.

(19) Varandas, A. J. C. *Conical Intersections: Electronic Structure, Dynamics & Spectroscopy*; Domcke, W., Yarkony, D. R., Köppel, H., Eds.; Advanced Series in Physical Chemistry, Vol. 15; World Scientific Publishing: River Edge, NJ, 2004; Chapter 5, p 91.

(20) Werner, H.-J.; Knowles, P. J. *J. Chem. Phys.* **1988**, *89*, 5803.

(21) Knowles, P. J.; Werner, H.-J. *Chem. Phys. Lett.* **1985**, *115*, 259.

(22) Werner, H.-J.; Knowles, P. J.; Almlöf, J.; Amos, R. D.; Deegan, M. J. O.; Elbert, S. T.; Hampel, C.; Meyer, W.; Peterson, K. A.; Pitzer, R.; Stone, A. J.; Taylor, P. R.; Lindh, R. *MOLPRO, a package of ab initio programs*; University College Cardiff Consultants Ltd.: Wales, U.K., 1998.

(23) Murrell, J. N.; Carter, S.; Farantos, S. C.; Huxley, P.; Varandas, A. J. C. *Molecular Potential Energy Functions;* Wiley: Chichester, U.K., 1984.

(24) Varandas, A. J. C. *Adv. Chem. Phys.* **1988**, *74*, 255.

(25) Varandas, A. J. C. *Lecture Notes in Chemistry*; Laganá, A., Riganelli, A., Eds.; Springer: Berlin, 2000; Vol. 75, pp 33.

(26) NIST Chemistry WebBook 69. http://webbook.nist.gov/chemistry (accessed 2003).

(27) Michels, H. H. *Adv. Chem. Phys.* **1981**, *45*, 225.

(28) San-Fabián, E.; Pastor-Abia, L. *Theor. Chem. Acc.* **2003**, *110*, 276.

(29) Bussery-Honvault, B.; Honvault, P.; Launay, J.-M. *J. Chem. Phys.* **2001**, *115*, 10701.

(30) Murrell, J. N.; Carter, S. *J. Phys. Chem.* **1984**, *88*, 4887.

(31) Varandas, A. J. C.; Poveda, L. A. *Theor. Chem. Acc.* **2006**, *116*, 404.

(32) Longuet-Higgins, H. C. *Proc. R. Soc. London, Ser. A* **1975**, *344*, 147.

(33) Varandas, A. J. C.; Tennyson, J.; Murrell, J. N. *Chem. Phys. Lett.* **1979**, *61*, 431.

(34) Matsunaga, N.; Yarkony, D. R. *J. Chem. Phys.* **1997**, *107*, 7825.

(35) Atchity, G. J.; Ruedenberg, K.; Nanayakkara, A. *Theor. Chem. Acc.* **1997**, *96*, 195.